Mikada, H., Moore, G.F., Taira, A., Becker, K., Moore, J.C., and Klaus, A. (Eds.)
Proceedings of the Ocean Drilling Program, Scientific Results Volume 190/196

1. Legs 190 and 196 Synthesis: Deformation and Fluid Flow Processes in the Nankai Trough Accretionary Prism[1]

Gregory F. Moore,[2] Hitoshi Mikada,[3] J. Casey Moore,[4]
Keir Becker,[5] and Asahiko Taira[6]

ABSTRACT

Ocean Drilling Program Legs 190 and 196 were a two-part program to study deformation and fluid flow in the central Nankai Trough off Shikoku Island. During Leg 190 two reference sites were drilled outboard of the trench (Sites 1173 and 1178), one site into the protothrust zone (Site 1174), two sites into a trench slope basin above a major out-of-sequence thrust (Sites 1175, 1176), and one site into an older portion of the accretionary prism. During Leg 196, Sites 1173 and 808 (drilled through the frontal thrust during Leg 131) were revisited, employing logging while drilling and installing two Advanced Circulation Obviation Retrofit Kits (ACORKs). Our reference sites defined the stratigraphic framework and physical properties baseline of the accreting/subducting Shikoku Basin sedimentary section. The proto-thrust and frontal thrust sites documented the dewatering and deformation processes at the toe of the accretionary prism. Porosity comparisons between Sites 1173 and 808 suggest that elevated fluid pressures occur beneath the décollement at Site 808. Initial measurements from the ACORK at Site 808 indicate a pressure pulse apparently from the décollement. Negative chloride anomalies at Sites 1174 and 808 could be due to fluid flow from deeper in the prism, but active smectite dehydration could also be responsible for the anomalies. Resistivity imaging of the frontal thrust shows borehole breakouts with principal stress orientations consistent with core-scale structures and plate convergence

[1]Moore, G.F., Mikada, H., Moore, J.C., Becker, K., and Taira, A., 2005. Legs 190 and 196 synthesis: deformation and fluid flow processes n the Nankai Trough accretionary prism. *In* Mikada, H., Moore, G.F., Taira, A., Becker, K., Moore, J.C., and Klaus, A. (Eds.), *Proc. ODP, Sci. Results,* 190/196, 1–26 [Online]. Available from World Wide Web: <http://www-odp.tamu.edu/publications/190196SR/VOLUME/SYNTH/SYNTH.PDF>. [Cited YYYY-MM-DD]
[2]Department of Geology and Geophysics, 1680 East-West Road, University of Hawaii, Honolulu HI 96822, USA. **gmoore@hawaii.edu**
[3]Department of Civil and Earth Resources Engineering, Kyoto University, Yoshida-Hommachi, Sakyo-ku, Kyoto 606-8501, Japan.
[4]Earth Sciences Department, University of California, Santa Cruz, Santa Cruz CA 95064, USA.
[5]Rosenstiel School of Marine and Atmospheric Science, University of Miami, 4600 Rickenbacker Causeway, Miami FL 33149, USA.
[6]Center for Deep Earth Exploration, Japan Agency for Marine-Earth Science and Technology (JAMSTEC), 2-15 Natushima-cho, Yokosuka 237-0061, Japan.

Initial receipt: 5 August 2004
Acceptance: 23 February 2005
Web publication: 18 May 2005
Ms 190SR-201

directions. Combined with a three-dimensional seismic reflection survey, our drilling data suggest that the décollement developed because of overpressuring beneath a diagenetic phase transition. Seismic data further suggest that the velocity-density inversion at the décollement at Sites 1174 and 808 is obliterated after underthrusting to seismogenic depths. The slope basin sites provide key evidence that the large out-of-sequence thrust was very recent and that the outer 40 km of the accretionary prism was built within the past 1 m.y.

INTRODUCTION

The Nankai Trough accretionary prism represents an "end-member" prism, accreting a thick terrigenous sediment section in a setting with structural simplicity and unparalleled resolution by seismic and other geophysical techniques. It therefore represents a superb setting for addressing the Ocean Drilling Program's (ODP's) Long Range Plan objectives for accretionary prism coring, in situ monitoring, and refinement of mechanical and hydrological models.

Legs 190 and 196 represent a two-part drilling program designed to measure the in situ physical properties and provide long-term monitoring of the physical and chemical states of the initial deformation along the subduction megathrust between the Philippine Sea and Eurasian plates in the central Nankai Trough (Fig. F1). Previously, Deep Sea Drilling Project (DSDP) Legs 31 and 87 and ODP Leg 131 drilling in this area, along with regional seismic reflection data, documented frontal offscraping and sediment dewatering at the toe of the accretionary prism. Although penetration was excellent and core recovery was very good, logging and installing borehole instrumentation were largely unsuccessful. A return to the Nankai Trough with advanced technology was thus enthusiastically endorsed by the ODP planning structure.

Leg 190 drilling included coring two reference sites, one in the Muroto Transect (Site 1173) and one in the Ashizuri Transect (Site 1177); one site in the protothrust zone off Muroto (Site 1174); and three slope sites off Muroto (Sites 1175, 1176, and 1178). Wireline logging was accomplished at Site 1173.

Leg 196 employed logging-while-drilling (LWD) technology, revisiting Sites 808 (originally drilled during Leg 131) and 1173. Advanced Circulation Obviation Retrofit Kits (ACORKs) were installed at both sites for long-term monitoring of in situ fluid pressures at multiple depths.

Geological and Geophysical Setting of Leg 190 and 196 Sites

The Nankai Trough is the subducting plate boundary between the Shikoku Basin and the southwest Japan arc (Eurasian plate) (Fig. F1). The Shikoku Basin is part of the Philippine Sea plate, which is subducting to the northwest under southwest Japan at a rate of 2–4 cm/yr, oriented ~310°–315° (Karig and Angevine, 1986; Seno et al., 1993) down an interface dipping 3°–7° (Kodaira et al., 2000). Repeated great earthquakes (magnitude > 8) with an average recurrence interval of ~180 yr (Ando, 1975) have occurred along the Nankai Trough throughout history. A sedimentary section ~1 km thick (Fig. F2) is accreted to or underthrust beneath the margin in the style of a fold and thrust belt at the

F1. Relief map of the Nankai Trough, p. 16.

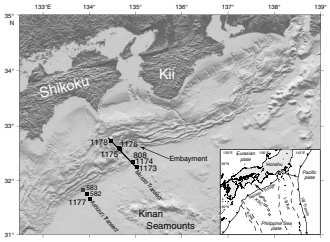

F2. Cross section along the Muroto Transect, p. 17.

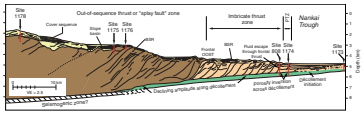

Nankai Trough, creating a large accretionary prism (Moore et al., 2001b).

Currently, the margin is locked, with convergence between Japan and the Philippine Sea plate stored locally as elastic stress (Mazzotti et al., 2000). The convergent margin of southwest Japan has a geologic record of accretion of deep-sea deposits extending to at least the Cretaceous (Taira et al., 1988). However, rocks cored during Leg 190 (Figs. **F1, F2**), even those subducted to seismogenic depths, entered the subduction zone no earlier than the Pliocene (Moore et al., 2001b).

In the area of Legs 190 and 196 drilling along the Muroto and Ashizuri Transects (Fig. **F1**), the sedimentary section at the basin-to-margin transition can be divided into the undeformed Shikoku Basin and overlying trench fill of the Nankai Trough, the protothrust zone, the imbricate thrust zone, and the out-of-sequence thrust (OOST) or "splay fault" zone (Fig. **F2**). A condensed summary of these tectonic provinces from Moore et al. (2001a) follows.

The Philippine Sea plate entering the Nankai Trough along the Muroto Transect is near the axis of an extinct spreading center marked by the Kinan Seamounts (Okino et al., 1994). As documented at Site 1173, the 16-Ma oceanic crust of the Shikoku Basin is overlain by, successively, volcaniclastic facies, middle Miocene to mid-Pliocene massive hemipelagic mudstones of the lower Shikoku Basin facies, upper Pliocene to lower Pleistocene hemipelagic mudstones with tephra layers (upper Shikoku Basin facies), a Pleistocene turbidite to hemipelagic facies transition sequence, and a Pleistocene to Holocene trench turbidite unit.

Subduction of the Kinan Seamounts has significantly modified the accretionary prism. The large embayment east of the Muroto Transect (Fig. **F1**) was caused by subduction of a particularly large seamount (Yamazaki and Okamura, 1989).

Entering the protothrust zone, the ~1-km-thick sedimentary section initially deforms above a protodécollement zone or incipient detachment surface developed in the uppermost Miocene massive hemipelagic mudstone layer. The lower part of this massive hemipelagic section is underthrust beneath the accretionary prism along with the underlying volcaniclastic sequence and oceanic crust. Coring at Site 1174 and seismic studies demonstrate that initial deformation in the protothrust zone (PTZ) consists of small thrust faults associated with subtle folding on scales well resolved in seismic profiles (Moore et al., 1990) and development of minor faults at core scales (Moore et al., 2001b; Morgan and Karig, 1995a).

Major thrust faulting and growth of the accretionary prism initiate at the frontal thrust and continue upslope (Fig. **F2**). Immediately landward of the frontal thrust, which was penetrated at Site 808, the imbricate thrust zone consists of a series of well-developed seaward-vergent imbricate packets spaced several kilometers apart. OOSTs overprint the imbricate thrusts, starting at the frontal OOST (Fig. **F2**). These OOSTs were probably initially imbricated from thick turbidite sand sequences of the Shikoku Basin (Moore et al., 2001b). The region upslope from the OOST zone is less well imaged than more seaward areas of the prism. However, the landward-dipping reflectors probably represent thrust boundaries and, in some cases, tilted sedimentary layering (**Ujiie et al.,** this volume). The 1946 Nankai Trough earthquake ruptured offshore of Kii Peninsula and Shikoku. Sites 1175, 1176, and 1178 are located close to the seaward limit of this rupture zone (Baba et al., 2002).

The Legs 190 and 196 drilling area shows high heat flow (Yamano et al., 2003) because the Muroto Transect is located near the extension of a ridge on the Philippine Sea plate (represented by the Kinan Seamounts) that ceased spreading at only 15 Ma. The young crust is blanketed by a thick sequence of sediment that restricts its convective cooling. Conductive heat flow values range from 180 mW/m² at Sites 1173 and 1174 (Shipboard Scientific Party, 2001a, 2001b) to 130 mW/m² at Site 808 (Shipboard Scientific Party, 1991). Heat flow values decrease rapidly upslope from the Nankai Trough, verifying the anomalously warm nature of the trench area (Yamano et al., 2003). The simple extrapolation of conductive heat flow with depth may overestimate temperature because of the potential of heat advection associated with fluid expulsion from the deforming sedimentary sequence. The temperatures at the top of oceanic crust at Sites 1173 and 808 were estimated at 110° and 120°C, respectively, by a conductive extrapolation of shallower measurements (Shipboard Scientific Party, 1991, 2001a). A less reliable extrapolation of only two very shallow data points at Site 1174 suggests a comparable basement temperature there (Shipboard Scientific Party, 2001b). Thus, the evidence indicates that basement temperatures exceed 100°C at Sites 1173, 1174, and 808. These high temperatures drive diagenetic reactions that significantly influence logging response.

RESULTS OF LEGS 190 AND 196

Seismic, Logging, and Core-Scale Structures and State of Stress

A terrigenous sediment-dominated subduction zone, such as the Nankai margin, should show horizontal shortening within the accretionary prism. The overall geometry of thrust faulting along this margin is apparent in seismic reflection profiles (Bangs et al., 2004; Gulick et al., 2004; Moore et al., 1990, 2001a; **Gulick and Bangs,** this volume); our view of this primary tectonic style is enhanced by detailed consideration of the information at seismic, logging, and core scales. Working from a seaward to landward direction, seismic profile and borehole data show a transition from extensional or basinal to a compressional stress regime.

The evidence for extensional deformation in the incoming sedimentary section of the Shikoku Basin is apparent at core, logging, and seismic profile scales. At Site 1173, fractures, as seen in cores and logs, are oriented at high angles, show normal displacement where measurable, and have variable strike orientation (Fig. **F3**) (Shipboard Scientific Party, 2001a, 2002b). Seismic data in this area reveal a pattern of normal faults within the incoming hemipelagic sediment with strikes statistically parallel to the margin and parallel to incoming highs in the oceanic crust (Fig. **F4**) (Heffernan et al., 2004). The patterns from the seismic data are more systematic than those observed in the borehole resistivity images, perhaps because the seismic data sample a larger sediment volume. To explain the extensional pattern of faulting, Heffernan et al. (2004) favored differential compaction both downdip of the subducting plate and off the flanks of the horsts in the oceanic crust.

The transition from a basinal or extensional regime to a compressional state of stress is obviously manifest at the PTZ, as seen in the seismic data where the seafloor begins to be subtly uplifted ~2 km seaward of the surface trace of the protothrust, indicating initiation of horizon-

F3. Poles to faults and fractures from RAB imaging, p. 18.

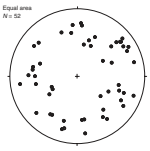

F4. Horst and graben structures on seismic image, p. 19.

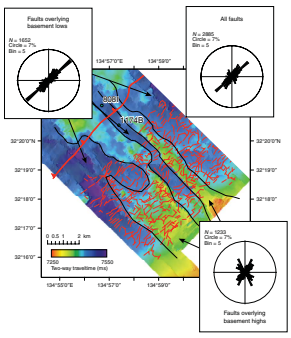

tal shortening (Fig. F5). The seaward extension of the décollement reflector also remains bright at this point, suggesting it may be an active surface of overpressuring and perhaps slip (Bangs et al., 2004). Cores from Site 1174 show well-developed deformation bands that indicate a horizontal maximum principal stress parallel to the direction of relative plate motion (Ujiie et al., 2004). A similar stress orientation was observed from analysis of numerous small-scale faults at Site 808 (Leg 131) (Lallemant et al., 1993). Borehole resistivity images at Site 808 show breakouts that indicate the maximum principal stress is oriented at ~N40°W, approximately parallel to the plate convergence direction (Fig. F6) (McNeill et al., 2004). Anisotropic orientation of formation resistivity derived from core sample measurements at Site 1174 indicates consistency with the direction of the plate convergence above the décollement zone (Henry et al., 2003). Thus, the geometry of the large-scale frontal thrusts plus the above-cited studies of cores and logs all indicate a maximum principal stress oriented parallel to the convergence direction (Seno et al., 1993).

Several studies concentrated on the permeability of the Nankai prism sediments (**Gamage and Screaton,** this volume; **Adatia and Maltman,** this volume; **Bourlange et al.,** this volume). Other laboratory studies quantified the stress state of the prism sediments (Kopf and Brown, 2003) and the consolidation of the clay-rich sedimentary sections (Karig and Ask, 2003). **Sunderland and Morgan** (this volume) documented microstructural variations in sediments of the prism toe.

Décollement Zone

Initiation of the Décollement Zone

The décollement zone separates the little-deformed underthrust material from the folded and thrusted offscraped and underplated rocks (Fig. F2). The décollement is the plate boundary and, therefore, how it develops and evolves is of significant interest. Near the deformation front of the accretionary prism, the décollement zone is characterized by a strong negative polarity seismic reflection (Bangs et al., 2004; Moore and Shipley, 1993). The décollement zone can be traced seaward as a bright reflector beyond the protothrust zone (Fig. F5). It locally bifurcates into several apparent splays near its seawardmost extent (Adamson, 2004). At Site 1173 the décollement zone, as observed at Sites 1174 and 808, stratigraphically projects into the lower Shikoku Basin deposits at ~400 m subbottom. No striking lithologic change occurs at this depth (Shipboard Scientific Party, 2001a). However, the onset of the smectite to illite phase transition does occur at this level (**Steurer and Underwood,** this volume a).

At Site 1173, physical property data from both logging and core measurements show minor changes in density and porosity at the depth of the projected décollement (Shipboard Scientific Party, 2001a, 2002b). Compressional velocities from cores and processed LWD data both show a reversal in the normally increasing trend with depth at the interval to which the décollement is projected at Site 1173 (Shipboard Scientific Party, 2001a; Yoneshima et al., 2003). This decrease in velocity may represent an increase in the elastic compressibility and a decrease in the rigidity of the sediment at this depth.

Bangs and Gulick (this volume) inverted the seismic reflection data for impedance and inferred porosity variations along one seismic line of the three-dimensional (3-D) seismic volume (Moore et al., 2001a).

F5. Stratigraphy and structure of prism toe of Muroto Transect, p. 20.

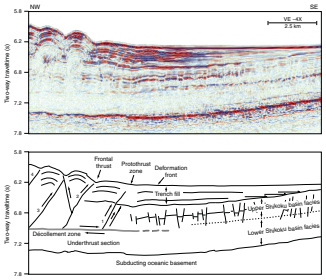

F6. Static-normalized RAB image for trench fill deposits, p. 21.

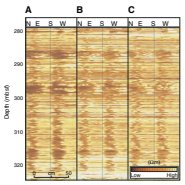

Based on the observed porosity variations, they argue that consolidation of the uppermost lower Shikoku Basin strata forms a barrier blocking fluid flow from the sediment section below that is consolidating because of loading by the trench turbidite fill. The barrier lies just above the projected level of the décollement, and they believe that higher-porosity, underconsolidated, and overpressured sediment below forms a surface of potential décollement propagation (Fig. F7).

Analysis of the microfabric of the décollement zone (Ujiie et al., 2003) indicates that it initiated in an interval of porous clayey sediment characterized by cementation due to intergranular bonding of authigenic clays. According to these authors, microstructures suggest (1) an initial phase of compactive deformation that involves the destruction of porous cement structure, probably caused by fluid pressure fluctuation, and (2) a later compactive deformation characterized by clay particle rotation and porosity collapse along slip surfaces, resulting in preferred orientation of clay particles. Studies of consolidation characteristics of the underthrust sediment (Morgan and Ask, 2004) also indicate a phase of early cementation and strengthening that may contribute to their mechanical coherency and propensity for underthrusting.

The role of fluid transport and/or high fluid pressure pervades concepts of décollement evolution (e.g., Saffer, 2003). Comparison of compaction curves between the reference Site 1173 and Site 808 at the frontal thrust suggests a fluid pressure, λ*, of 0.42 below the décollement zone at the latter site (Screaton et al., 2002):

$$\lambda^* = \frac{\text{(pore pressure – hydrostatic pressure)}}{\text{(lithostatic pressure – hydrostatic pressure)}}.$$

LWD resistivity data (Bourlange et al., 2003) and porosity data in the décollement zone suggest higher fluid pressures and high permeabilities in this fractured interval. Thus, the décollement zone may represent a preferential interval of fluid transport from higher pressure sources.

Based on geochemical data, the décollement zone has been considered as a locus of episodic fluid flow (Kastner et al., 1993; Spivack et al., 2002). However, recent analyses of clay mineral composition and associated modeling suggest that the large negative chloride anomaly in the vicinity of the Nankai décollement zone may be explained by smectite dehydration (Brown et al., 2001; Henry and Bourlange, 2004). The explanation of the low chloride anomaly by clay dehydration does not preclude lateral flow or overpressure within the décollement zone but simply eliminates the use of the chloride anomaly as an indicator of flow.

The preponderance of evidence suggests that the décollement zone develops because of initial overpressuring and perhaps extensional fracturing succeeded by a shear, an idea that emerged from the Leg 131 results (Karig and Morgan, 1994; Morgan and Karig, 1995a). Propagation of the décollement zone in a relatively homogeneous sedimentary section is puzzling. However, the development of a hydrologically resistive barrier caused by dewatering of the uppermost lower Shikoku Basin unit or to intrinsically low vertical permeability provides a reasonable explanation.

Evolution of the Décollement Zone

The evolution of the décollement zone can be evaluated using information available from the two boreholes that penetrated it and from in-

F7. Consolidation model for upper and lower Shikoku Basin facies, p. 22.

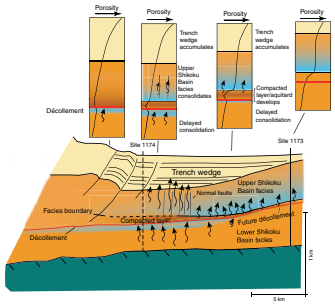

ferences gained through study of the 3-D seismic volume (Fig. F2). Both Sites 1174 and 808 indicate a significant downsection porosity inversion due to underthrusting of the lower Shikoku Basin deposits at a rate faster than they can dewater, thus resulting in overpressures. This inversion in physical properties produces a strong negative polarity reflection beneath Sites 808 and 1174 (Moore and Shipley, 1993; Bangs et al., 2004). The amplitude of the negative reflection declines in a landward direction so that the reflection between the offscraped and underthrust sediment sections diminishes to very low amplitude. The décollement steps down to the oceanic crust ~40 km landward of the deformation front, thus underplating the remaining sediment on the subducting plate (Bangs et al., 2004; Moore et al., 2001a). The declining amplitude is consistent with dewatering and consolidation of the underthrust section. In addition to escaping through intergranular permeability, the fracture permeability of the thrust faults overlying the décollement zone may act as fluid escape paths (Gulick et al., 2004).

ACORK Installations

In 2001, multilevel ACORKs were installed in Holes 1173B and 808I during Leg 196. These ACORKs were configured to provide long-term (10 yr or longer) monitoring of in situ fluid pressures at five depth intervals in Hole 1173B, including basement, and six depth intervals in Hole 808I, including the décollement zone. Details of the installations are described in Mikada, Becker, Moore, Klaus, et al. (2002). A significant installation flaw in the ACORK set at 922 meters below seafloor (mbsf) in Hole 808I resulted from the inability to drill the final ~37 m above the décollement zone. This circumstance precluded installation of a bridge plug to make the final seal of the deepest monitoring interval just above the décollement zone.

Since Leg 196, the ACORKs have been revisited annually with ships and submersibles from the Japan Marine Science and Technology Center (JAMSTEC), including the remotely operated vehicle (ROV) *Kaiko* in 2002 and 2003 and the submersible *Shinkai* 6500 in 2004. *Kaiko* operations in 2002 (Mikada et al., 2003) showed that the majority of sampling valves had somehow worked open during the Leg 196 installation operations a year earlier (perhaps caused by current-induced vibrations); the *Kaiko* was used to close the valves in 2002, but the recovered data were not useful scientifically. The *Kaiko* revisit in 2003 was intended to collect a year of data and install a bridge plug within the top of casing in Hole 808I, but these objectives were left unfulfilled when the *Kaiko* vehicle was catastrophically lost at the end of the first dive. In late spring of 2004, two dives with the *Shinkai* 6500 collected the first useful pressure data from both ACORKs. However, the limited bottom time did not allow installation of the bridge plug in Hole 808I, which must await a future submersible operation.

Preliminary inspection of the data collected in 2004 shows that, despite the lack of full seal in the décollement interval, the ACORK in Hole 808I captured the signal of a July 2003 solitary pressure wave that seems to have originated in the décollement zone (Fig. F8). Interpretation of this event as well as determination of background in situ fluid pressures is ongoing as this synthesis is being written (Davis et al., submitted [N1]). At this time it should be cautioned that the signal is that of a pressure transient; it does not necessarily imply any significant fluid flow. The fact that signals like these are being recorded

F8. Pressure time series recorded by ACORK in Hole 808I, p. 23.

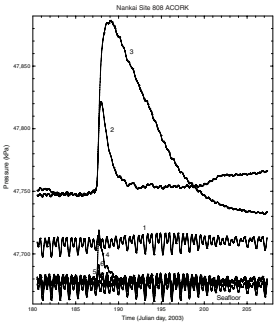

demonstrates the long-term usefulness of the ACORK installations despite any original installation flaws.

Microbiology

Core samples obtained at Sites 1173, 1174, 1176, and 1177 were analyzed for microbiology using polymerase chain reaction (PCR) amplification, genetic analyses, and other standard techniques. The counts of bacteria are close to predicted values for deep ocean sediment at Site 1177 and at the shallower depths of Sites 1173 and 1174. However, the total counts of bacteria for depths deeper than 400–500 mbsf at Sites 1173 and 1174 show very low numbers. Sequences of bacteria within the core samples were similar to others retrieved from marine sediment and other anoxic habitats, and so probably represent important indigenous bacteria (Toffin et al., 2004a, 2004b; Webster et al., 2003, 2004; Zink et al., 2003). Analysis suggests limited methanogen diversity with only three gene clusters identified within the *Methanosarcinales* and *Methanobacteriales*. The cultivated members of the *Methanobacteriales* and some of the *Methanosarcinales* can use H_2 and CO_2 to produce methane (Newberry et al., 2004). These counts might be influenced by the temperature gradients in the sediments at Sites 1173 and 1174. Members of the genus *Thermococcus,* which in general live in 48°–73°C environments, are found at Site 1176, where in situ temperature ranges 1°–12°C. The *Thermococcus* populations thus are presumably not metabolically active in situ. They could represent either inactive relict cells introduced by past hydrothermal activity or cells that were recently introduced through interstitial fluid flow (Kormas et al., 2003).

Tectonics and Sedimentation

Subducting Sedimentary Section

The Shikoku Basin sedimentary section dewaters as it underthrusts the Nankai accretionary prism. Legs 190 and 196 drilling documented significant along- and across-strike variations in the physical, geochemical, and sedimentologic properties of the subducting section that influence its compaction and dewatering (e.g., **Steurer and Underwood,** this volume b; **Hoffman and Tobin,** this volume; **Goldberg et al.,** this volume).

The upper Shikoku Basin facies (Pliocene–Quaternary) drilled at Sites 1173, 1174, and 1177 was deposited by hemipelagic settling and ash falls; the lower Shikoku Basin facies (Pliocene–middle Miocene) is also a dominantly hemipelagic sequence but lacks recognizable ash layers (Shipboard Scientific Party, 2001c). The lower Shikoku Basin section at Site 1177 drilled along the Ashizuri Transect contains abundant siliciclastic sand layers with rare beds of gravel and mudstone-clast conglomerate, whereas the lower Shikoku Basin section off Muroto (Sites 1173 and 1174) does not contain turbidite layers.

Lower–upper Miocene turbidite beds of the lower Shikoku Basin section at Site 1177 were derived from a continental source with exposed plutonic and volcanic rocks, possibly the inner zone of southwest Japan (**Fergusson,** this volume). Turbidite sand was transported across the trench and at least 600 km out onto the Shikoku Basin plain. The turbidites were interbedded with hemipelagic layers in topographic lows, while topographic highs did not receive any turbidity current deposits and were thus dominated by hemipelagic deposits. Similar composi-

tions are present in the thick sand packages of the lower–upper Miocene accreted trench deposits at Site 1178. The thrust slices penetrated at Site 1178 are 400–600 m thick, indicating that the trench was accumulating large amounts of terrigenous sediment at that time.

Clay mineral data from Sites 1173, 1174, and 1177 show downhole increases in smectite percentage within the Shikoku Basin deposits. Part of this increase is caused by changes in detrital influx, but diagenetic reactions also affect these hemipelagic sequences. **Steurer and Underwood** (this volume a) conclude that recent episodes of burial near the toe of the Nankai accretionary prism (i.e., by trench-axis sedimentation, tectonic thickening, and frontal thrusting) may have been too fast for the smectite-illite reaction to keep pace. The sedimentation rate of smectite in the Shikoku Basin and Nankai Trough was higher during the Miocene and decreased progressively through the Pliocene and Quaternary. In situ alteration of disseminated volcanic glass added even more authigenic smectite to the clay assemblage as burial depths and temperatures gradually increased. The geothermal gradient at Site 1177 is substantially lower than at Sites 1173 and 1174; consequently, volcanic ash alters to smectite in lower Shikoku Basin deposits but smectite-illite diagenesis has not started along the Ashizuri Transect (Moore et al., 2001b; **Wilson et al.,** this volume; **Underwood et al.,** this volume). The absolute abundance of smectite in mudstone from Site 1177 is sufficient (30–60 wt%) to influence the strata's shear strength and hydrogeology as it subducts along the Ashizuri Transect (**Steurer and Underwood,** this volume a).

Trench and Trench Slope Deposits

Deposition of the upper part of the Miocene turbidite succession at Site 1177 was synchronous with deposition of the uplifted and deformed axial and outer trench wedge facies at Site 1178 (Fig. **F1**) (Shipboard Scientific Party, 2001c). Sand beds at both sites have low quartz content but contain a significant component of sedimentary and metamorphic rock fragments (**Fergusson,** this volume) that were derived mainly from older accretionary complexes (e.g., Sambagawa and Shimanto Belts) of southwest Japan (Outer Belt) (Fig. **F9**). These sand beds contrast with those of the modern trench deposits that are derived from the Izu collision zone of eastern Honshu (Taira and Niitsuma, 1986).

Trench slope basin sand beds drilled at Sites 1175 and 1176 contain abundant sedimentary lithic fragments as well as radiolarian chert fragments, indicating that they were derived from erosion of the Shimanto accretionary complex on Shikoku Island (**Fergusson,** this volume). The eroded material was delivered to the slope basins via submarine canyons that incised the landward trench slope southeast of Shikoku Island (Underwood et al., 2003; **Underwood and Steurer,** this volume).

Organic geochemical studies have been performed on the clay-rich slope sediments by **Yamamoto** (this volume) and **Suzuki et al.** (this volume).

Evolution and Rapid Growth of the Accretionary Prism

Although definitive proof is lacking, the lines of evidence listed by Taira (2001) indicate that the present phase of north-northwest–trending subduction of the Philippine Sea plate started at ~8 Ma. As discussed above, topographic lows in the Shikoku Basin were filled by a turbidite sequence derived from the Outer Belt of Shikoku (Fig. **F9**). In contrast,

F9. Sedimentary and structural evolution of the central Nankai Trough, p. 24.

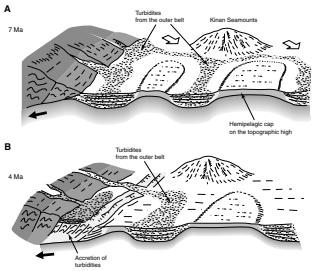

around the Kinan Seamount chain, the higher seamount peaks stood above the cloud of fine-grained turbidite sedimentation, although topographic highs with lower relief were also buried by turbidites and fine-grained hemipelagic sediments. Accretion of these turbidite units at the Muroto Transect by 4 Ma produced an accretionary complex mainly composed of turbidites derived from the Outer Belt (Site 1178). By 2 Ma, further accretion of these turbidite units (Sites 1175 and 1176) and indentation of the accretionary prism by a seamount reshaped the morphology of the landward slope. At the same time, in the Izu collision zone that marks the eastern end of the Nankai Trough, active tectonism produced mountain-to-trough sediment transport, leading to domination by axial channel depositional systems in the Nankai Trough. From ~1 Ma to the present (Fig. F9), accretion of the axial trench wedge and underthrusting of the hemipelagic cap of the Kinan Seamounts in the embayment produced by seamount subduction dominated the present-day tectono-sedimentary framework of the toe part of the Muroto Transect (Sites 808, 1174, and 1173).

One of the more significant discoveries during Leg 190 is the age of accreted trench turbidites at Sites 1175 and 1176. Underwood et al. (2003) interpret contact relations between trench slope sediments and underlying accreted trench deposits to indicate that the youngest accreted turbidites are only ~1 Ma. These sites are located 40 km landward of the frontal thrust. If we assume steady-state seaward growth of the prism over the past 1 m.y., the lateral growth rate is 40 km/m.y. Even if the actual slope-to-prism contact is deeper (and thus somewhat older), the rate of tectonic accretion remains impressive. In comparison, the turbidite-rich Middle America accretionary prism off the coast of Mexico has grown ~23 km in width during the past 10 m.y. (Moore et al., 1982) and the eastern Aleutian accretionary prism has grown 20 km in 3 m.y. (von Huene et al., 1998).

Summary

Analyses of core and logging data collected in a series of drill holes in the sediments of the Shikoku Basin, Nankai Trough, and flanking accretionary wedge, interpreted along with seismic reflection data, reveal details of deformation and fluid flow within the Nankai subduction zone. LWD acquired spectacular physical property data and images of unconsolidated sediments in spite of unstable hole conditions. Two holes along the Muroto Transect were instrumented with ACORKs for long-term monitoring of fluid pressure in and around the décollement zone.

Major results include the following:

1. Seismic and borehole data show a transition from extensional to a compressional stress regime from a seaward to landward direction across the deformation front. Seaward of the deformation front, faults show normal displacement with variable strike orientation. Landward of the deformation front compressional orientation produces structures at core, logging, and seismic profile scales consistent with the convergence of the Philippine Sea plate.
2. The young, hot, subducting Philippine Sea plate along the Muroto Transect probably caused smectite dehydration in the vicinity of the décollement zone. The large negative chloride anomaly at the décollement may be produced by a diagenetic reaction.

Thus, episodic flow of low-chloride fluids from the deeper part of the subduction zone is not required.

3. Initiation of the décollement might be controlled by trench sediment loading of the lower Shikoku Basin deposits and fluid pressure rise beneath a diagenetic front. The high fluid pressure may initiate décollement development by extensional fracturing of the lower Shikoku basin deposits.
4. Dating slope and accreted trench deposits of the Nankai Trough inner slope indicates that a large OOST was formed very recently and the outer 40 km of the accretionary prism was built within the past 1 m.y. The Nankai accretionary complex developed rapidly compared to the other subduction zones.

The results of Legs 190 and 196 clearly demonstrate that fluid has played a major role in the formation and evolution of the Nankai accretionary prism. Because deep-sourced fluids are critical to understanding seismogenic processes, it is important to obtain results from long-term fluid pressure measurements. Further understanding the Nankai seismogenic zone requires deeper drilling into faults active during past great earthquakes.

ACKNOWLEDGMENTS

This research used samples and data provided by the Ocean Drilling Program (ODP). ODP is sponsored by the U.S. National Science Foundation (NSF) and participating countries under management of Joint Oceanographic Institutions (JOI), Inc. Funding for this research was provided by the U.S. Science Support Program (USSSP), by the Ministry of Education, Science, Culture and Sports of Japan (MEXT) as the Grant-in-Aid for Scientific Research for the Ocean Drilling Program, by the Ocean Research Institute of the University of Tokyo, and by the Japan Agency for Marine-Earth Science and Technology (JAMSTEC). We acknowledge software grants from Landmark Graphics Corporation with which G.F. Moore and J.C. Moore processed and displayed seismic reflection data used on Legs 190 and 196, including Figures F4 and F5 herein. We thank Earl Davis for reviewing a draft of this paper and for providing Figure F8. ODP reviewers Don Fisher and Dave Scholl provided extremely useful comments that helped to clarify the text. We gratefully acknowledge the hard work by the publications staff at ODP-TAMU. Many thanks are also due to Adam Klaus, our Staff Scientist on both legs, for his help in making this program a success. This manuscript is SOEST contribution number 6520.

REFERENCES

Adamson, S., 2004. Controls on the morphological variability of the décollement zone in the Nankai Trough subduction zone [M.S. thesis]. Univ. California, Santa Cruz.

Ando, M., 1975. Source mechanisms and tectonic significance of historical earthquakes along the Nankai Trough, Japan. *Tectonophysics,* 27:119–140.

Baba, T., Uhira, K., Tanioka, Y., and Cummins, P.R., 2002. The slip distribution of the 1946 Nankai earthquake estimated from tsunami inversion using a new plate model. *Phys. Earth Planet. Int.,* 132:59–73.

Bangs, N.L.B., Shipley, T.H., Gulick, S.P.S., Moore, G.F., Kuromoto, S., and Nakamura, Y., 2004. Evolution of the Nankai Trough décollement from the trench into the seismogenic zone: inferences from three-dimensional seismic reflection imaging. *Geology,* 32:273–276.

Bourlange, S., Henry, P., Moore, J.C., Mikada H., and Klaus, A., 2003. Fracture porosity in the décollement zone of Nankai accretionary wedge using logging-while-drilling resistivity data. *Earth Planet. Sci. Lett.,* 209:103–112.

Brown, K.M., Saffer, D.M., and Bekins, B.A., 2001. Smectite diagenesis, pore-water freshening, and fluid flow at the toe of the Nankai wedge. *Earth Planet. Sci. Lett.,* 194:97–109.

Gulick, S.P.S., Bangs, N.L.B., Shipley, T.H., Nakamura, Y., Moore, G., and Kuramoto, S., 2004. Three-dimensional architecture of the Nankai accretionary prism's imbricate thrust zone off Cape Muroto, Japan: prism reconstruction via en echelon thrust propagation. *J. Geophys. Res.,* 109:10.1029/2003JB002654.

Heffernan, A.S., Moore, J.C., Bangs, N.L., Moore, G.F., and Shipley, T.H., 2004. Initial deformation in a subduction thrust system: polygonal normal faulting in the incoming sedimentary sequence of the Nankai subduction zone, southwestern Japan, application to the exploration of sedimentary basins. *In* Davies, R.J., et al. (Eds.), *3D Seismic Technology: Application to the Exploration of Sedimentary Basin.* Mem.—Geol. Soc. London, 29:143–148.

Henry, P., and Bourlange, S., 2004. Smectite and fluid budget at Nankai ODP sites derived from cation exchange capacity. *Earth Planet. Sci. Lett.,* 219:129–145.

Henry, P., Jouniaux, L., Screaton, E.J., Hunze, S., and Saffer, D.M., 2003. Anistropy of electrical conductivity record of initial strain at the toe of the Nankai accretionary wedge. *J. Geophys. Res.,* 108:10.1029/2002JB002287.

Karig, D.E., and Angevine, C.L., 1986. Geologic constraints on subduction rates in the Nankai Trough. *In* Kagami, H., Karig, D.E., and Coulbourn, W.T., et al., *Init. Repts. DSDP,* 87: Washington (U.S. Govt. Printing Office), 789–796.

Karig, D.E., an Ask, M.V.S., 2003. Geological perspectives on consolidation of clay-rich marine sediments. *J. Geophys.Res.,* 108:10.1029/2001JB000652.

Karig, D.E., and Morgan, J.K., 1994. Tectonic deformation: stress paths and strain histories. *In* Maltman, A. (Ed.), *The Geological Deformation of Sediments:* London (Chapman and Hall), 167–204.

Kastner, M., Elderfield, H., Jenkins, W.J., Gieskes, J.M., and Gamo, T., 1993. Geochemical and isotopic evidence for fluid flow in the western Nankai subduction zone, Japan. *In* Hill, I.A., Taira, A., Firth, J.V., et al., *Proc. ODP, Sci. Results,* 131: College Station, TX (Ocean Drilling Program), 397–413.

Kodaira, S.N.T., Park, J.O., Mochizuki, K., Shinohara, M., and Kimura, S., 2000. Western Nankai Trough seismogenic zone: results from a wide-angle ocean bottom seismic survey. *J. Geophys. Res.,* 105:5887–5906.

Kopf, A., and Brown, K.M., 2003. Friction experiments on saturated sediments and their implications for the stress state of the Nankai and Barbados subduction thrusts. *Mar. Geol.,* 202:193–210.

Kormas, K.A., Smith, D.C., Edgcomb, V., and Teske, A., 2003. Molecular analysis of deep subsurface microbial communities in Nankai Trough sediments (ODP Leg 190, Site 1176A). *FEMS Microbiol. Ecol.,* 45:115–125.

Lallemant, S.J., Byrne, T., Maltman, A., Karig, D., and Henry, P., 1993. Stress tensors at the toe of the Nankai accretionary prism: an application of inverse methods to slickenlined faults. *In* Hill, I.A., Taira, A., Firth, J.V., et al., *Proc. ODP, Sci. Results,* 131: College Station, TX (Ocean Drilling Program), 103–122.

Mazzotti, S., LePichon, X., Henry, P., and Miyazaki, S., 2000. Full interseismic locking of the Nankai and Japan-West Kuril Subduction Zones: an analysis of uniform elastic strain accumulation in Japan constrained by permanent GPS. *J. Geophys. Res.,* 105:13159–13177.

McNeill, L.C., Ienaga, M., Tobin, H., Saito, S., Goldberg, D., Moore, J.C., and Mikada, H., 2004. Deformation and in situ stress in the Nankai accretionary prism from resistivity-at-bit images, ODP Leg 196. *Geophys. Res. Lett.,* 31:10.1029/2003GL018799.

Mikada, H., Becker, K., Moore, J.C., Klaus, A., et al., 2002. *Proc. ODP, Init. Repts.,* 196 [CD-ROM]. Available from: Ocean Drilling Program, Texas A&M University, College Station TX 77845-9547, USA.

Mikada, H., Kinoshita, M., Becker, K., Davis, E.E., Meldrum, R.D., Flemings, P., Gulick, S.P.S., Matsubayashi, O., Morita, S., Goto, S., Misawa, N., Fujino, K., and Toizumi, M., 2003. Hydrologeological and geothermal studies around Nankai Trough (KR02-10 Nankai Trough cruise report). *JAMSTEC J. Deep Sea Res.,* 22:125–171.

Moore, G.F., and Shipley, T.H., 1993. Character of the décollement in the Leg 131 area, Nankai Trough. *In* Hill, I.A., Taira, A., Firth, J.V., et al., *Proc. ODP, Sci. Results,* 131: College Station, TX (Ocean Drilling Program), 73–82.

Moore, G.F., Shipley, T.H., Stoffa, P.L., Karig, D.E., Taira, A., Kuramoto, S., Tokuyama, H., and Suyehiro, K., 1990. Structure of the Nankai Trough accretionary zone from multichannel seismic reflection data. *J. Geophys. Res., [Solid Earth Planets],* 95:8753–8765.

Moore, G.F., Taira, A., Bangs, N.L., Kuramoto, S., Shipley, T.H., Alex, C.M., Gulick, S.S., Hills, D.J., Ike, T., Ito, S., Leslie, S.C., McCutcheon, A.J., Mochizuki, K., Morita, S., Nakamura, Y., Park, J.O., Taylor, B.L., Toyama, G., Yagi, H., and Zhao, Z., 2001a. Data report: Structural setting of the Leg 190 Muroto Transect. *In* Moore, G.F., Taira, A., Klaus, A., et al., *Proc. ODP, Init. Repts.,* 190 [Online]. Available from World Wide Web: <http://www-odp.tamu.edu/publications/190_IR/chap_02/chap_02.htm>.

Moore, G.F., Taira, A., Klaus, A., and Leg 190 Scientific Party, 2001b. New insights into deformation and fluid flow processes in the Nankai Trough accretionary prism: results of Ocean Drilling Program Leg 190. *Geochem., Geophys., Geosyst.,* 2:10.1029/2001GC000166.

Moore, J.C., Watkins, J.S., Shipley, T.H., McMillen, K.J., Bachman, S.B., and Lundberg, N., 1982. Geology and tectonic evolution of a juvenile accretionary terrane along a truncated convergent margin: synthesis of results from Leg 66 of the Deep Sea Drilling Project, southern Mexico. *Geol. Soc. Am. Bull.,* 93:847–861.

Morgan, J.K., and Ask, M.V.S., 2004. Consolidation state and strength of underthrust sediments and evolution of the décollement at the Nankai accretionary margin: results of uniaxial reconsolidation experiments. *J. Geophys. Res.,* 109:10.1029/2002JB002335.

Morgan, J.K., and Karig, D.E., 1995a. Décollement processes at the Nankai accretionary margin, southeast Japan. *J. Geophys. Res.,* 100:15221–15231.

Newberry, C.J., Webster, G., Cragg, B.A., Parkes, R.J., Weightman, A.J., and Fry, J.C., 2004. Diversity of prokaryotes and methanogenesis in deep subsurface sediments from the Nankai Trough, Ocean Drilling Program Leg 190. *Environ. Microbiol.,* 6:274–287.

Okino, K., Shimakawa, Y., and Nagaoka, S., 1994. Evolution of the Shikoku Basin. *J. Geomagn. Geoelectr.,* 46:463–479.

Saffer, D.M., 2003. Pore pressure development and progressive dewatering in underthrust sediments at the Costa Rican subduction margin: comparison with northern Barbados and Nankai. *J. Geophys. Res.*, 108:10.1029/2002JB0001787.

Screaton, E., Saffer, D., Henry, P., Hunze, S., Moore, G.F., Taira, A., Klaus, A., Becker, K., Becker, L., Boeckel, B., Cragg, B.A., Dean, A., Fergusson, C.L., Hirano, S., Hisamitsu, T., Kastner, M., Maltman, A.J., Morgan, J.K., Murakami, Y., Sanchez-Gomez, M., Smith, D.C., Spivack, A.J., Steurer, J., Tobin, H.J., Ujiie, K., Underwood, M.B., and Wilson, M., 2002. Porosity loss within the underthrust sediments of the Nankai accretionary complex: implications for overpressures. *Geology,* 30(1):19–22.

Seno, T., Stein, S., and Gripp, A.E., 1993. A model for the motion of the Philippine Sea plate consistent with NUVEL-1 and geological data. *J. Geophys. Res.,* 98:17941–17948.

Shipboard Scientific Party, 1991. Site 808. *In* Taira, A., Hill, I., Firth, J.V., et al., *Proc. ODP, Init. Repts.,* 131: College Station, TX (Ocean Drilling Program), 71–269.

Shipboard Scientific Party, 2001a. Site 1173. *In* Moore, G.F., Taira, A., Klaus, A., et al., *Proc. ODP, Init. Repts.,* 190 [Online]. Available from World Wide Web: <http://www-odp.tamu.edu/publications/190_IR/chap_04/chap_04.htm>.

Shipboard Scientific Party, 2001b. Site 1174. *In* Moore, G.F., Taira, A., Klaus, A., et al., *Proc. ODP, Init. Repts.,* 190 [Online]. Available from World Wide Web: <http://www-odp.tamu.edu/publications/190_IR/chap_05/chap_05.htm>.

Shipboard Scientific Party, 2001c. Site 1177. *In* Moore, G.F., Taira, A., Klaus, A., et al., *Proc. ODP, Init. Repts.,* 190 [Online]. Available from World Wide Web: <http://www-odp.tamu.edu/publications/190_IR/chap_08/chap_08.htm>.

Shipboard Scientific Party, 2002a. Site 1173. *In* Mikada, H., Becker, K., Moore, J.C., Klaus, A., et al., *Proc. ODP, Init. Repts.,* 196, 1–97 [Online]. Available from World Wide Web: http://www-odp.tamu.edu/publications/196_IR/VOLUME/CHAPTERS/IR196_03.PDF.

Shipboard Scientific Party, 2002b. Site 808. *In* Mikada, H., Becker, K., Moore, J.C., Klaus, A., et al., *Proc. ODP, Init. Repts.,* 196, 1–68 [Online]. Available from World Wide Web: http://www-odp.tamu.edu/publications/196_IR/VOLUME/CHAPTERS/IR196_04.PDF.

Spivack, A.J., Kastner, M., and Ransom, B., 2002. Elemental and isotopic chloride geochemistry and fluid flow in the Nankai Rough. *Geophys. Res. Lett.,* 29:10.1029/2001GL014122.

Taira, A., 2001. Tectonic evolution of the Japanese Island arc system. *Annu. Rev. Earth Planet. Sci.,* 29:109–134.

Taira, A., Katto, J., Tashiro, M., Okamura, M., and Kodama, K., 1988. The Shimanto Belt in Shikoku, Japan: evolution of Cretaceous to Miocene accretionary prism. *Mod. Geol.,* 12:5–46.

Taira, A., and Niitsuma, N., 1986. Turbidite sedimentation in the Nankai Trough as interpreted from magnetic fabric, grain size, and detrital modal analyses. *In* Kagami, H., Karig, D.E., Coulbourn, W.T., et al., *Init. Repts. DSDP,* 87: Washington (U.S. Govt. Printing Office), 611–632.

Toffin, L., Bidault, A., Pignet, P., Tindall, B.J., Slobodkin, A., Kato, C., and Prieur, D., 2004. *Shewanella profunda* sp. nov., isolated from deep marine sediment of the Nankai Trough. *Int. J. Syst. Evol. Microbiol.,* 54:1943–1949.

Toffin, L., Webster, G., Weightman, A.J., Fry, J.C., and Prieur, D., 2004. Molecular monitoring of culturable bacteria from deep sea sediment of the Nankai Trough, Leg 190 Ocean Drilling Program. *FEMS Microbiology Ecology,* 48:357–367.

Ujiie, K., Hisamitsu, T., and Taira, A., 2003. Deformation and fluid pressure variation during initiation and evolution of the plate boundary décollement zone in the Nankai accretionary prism. *J. Geophys. Res., [Solid Earth],* 108:10.1029/2002JB002314.

Ujiie, K., Maltman, A.J., and Sánchez-Gómez, M., 2004. Origin of deformation bands in argillaceous sediments at the toe of the Nankai accretionary prism, southwest Japan. *J. Struct. Geol.,* 26:221–231.

Underwood, M.B., Wilson, M.E.J., Fergusson, C.L., Hirano, S., Steurer, J., Becker, K., Becker, L., Boeckel, B., Cragg, B., Dean, A., Henry, P., Hisamitsu, T., Hunze, S., Kastner, M., Maltman, A., Morgan, J., Murakami, Y., Saffer, D., Sanchez-Gómez, M., Screaton, E., Smith, D., Spivak, A., Tobin, H., Ujiie, K., Moore, G.F., Taira, A., and Klaus, A., 2003. Sedimentary and tectonic evolution of a trench-slope basin in the Nankai subduction zone of southwest Japan. *J. Sediment. Res.,* 73:589–602.

von Huene, R., Klaeschen, D., Gutscher, M., and Fruehn, J., 1998. Mass and fluid flux during accretion at the Alaskan margin. *Geol. Soc. Am. Bull.,* 110:468–482.

Webster, G., Newberry, C.J., Fry, J.C., and Weightman, A.J., 2003. Assessment of bacterial community structure in the deep sub-seafloor biosphere by 16S RDNA-based techniques: a cautionary tale. *J. Microbiol. Methods,* 55:155–164.

Webster, G., Parkes, R.J., Fry, J.C., and Weightman, A.J., 2004. Widespread occurrence of a novel division of bacteria identified by 16S rRNA gene sequences originally found in deep marine sediments. *Appl. Environ. Microbiol.,* 70:5708–5713.

Yamano, M., Kinoshita, M., Goto, S., and Matsubayashi, O., 2003. Extremely high heat flow anomaly in the middle part of the Nankai Trough. *Phys. Chem. Earth, [Solid Earth Geod.],* 28:487–497.

Yamazaki, T., and Okamura, Y., 1989. Subducting seamounts and deformation of overriding forearc wedges around Japan. *Tectonophysics,* 160:207–229.

Yoneshima, S., Endo, T., Pistre, V., Thompson, J., Campanac, P., Mikada, H., Moore, J.C., Ienaga, M., Saito, S., and Leg 196 Scientific Party, 2003. Processing leaky-compressional mode from LWD sonic data in shallow ocean sediments: ODP sites in Nankai Trough. *Proc. 6th SEGJ Int. Symp.: Imaging Technology:* Tokyo (Soc. Expl. Geophys. Jpn.), 45–52.

Zink, K.-G., Wilkes, H., Disko, U., Elvert, M., and Horsfield, B., 2003. Intact phospholipids—microbial "life markers" in marine deep subsurface sediments. *Org. Geochem.*, 34:755–769.

Figure F1. Shaded relief map of the Nankai Trough, produced from the Hydrographic Department of Japan's topographic data set (500-m grid interval), showing the regional setting of the Leg 190 and 196 drill sites as well as sites drilled during Leg 87 (Sites 582 and 583). Line through drill sites in Muroto Transect shows location of generalized cross section of Figure F2, p. 17. The inset is a tectonic map of the Philippine Sea region that includes the Nankai Trough. I-B Trench = Izu-Bonin Trench, KPR = Kyushu-Palau Ridge, KSC = Kinan Seamount Chain (fossil spreading center).

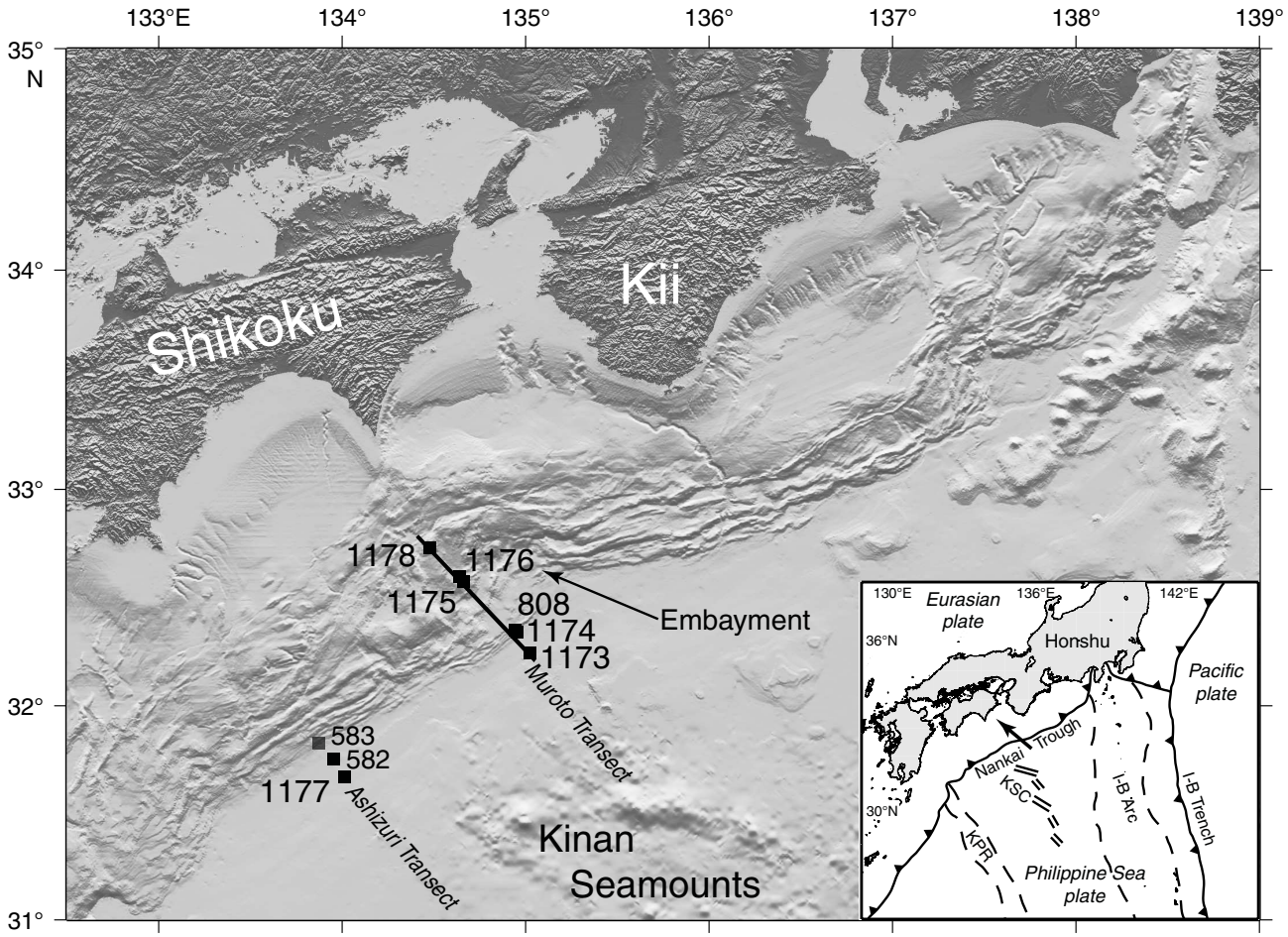

Figure F2. Generalized cross section along the Muroto Transect along the line shown on Figure F1, p. 16. OOST = out-of-sequence thrust, PTZ = protothrust zone, BSR = bottom-simulating reflector, VE = vertical exaggeration. Major observations pertinent to décollement evolution are shown. After initiation of the décollement as outlined in Figure F5, p. 20, the underthrusting of the lower Shikoku Basin sediment creates a porosity inversion as observed at Sites 1174 and 808 and a strong negative polarity reflection. Amplitude loss with continued underthrusting apparently reflects consolidation of the sediments below the décollement (Bangs et al., 2004).

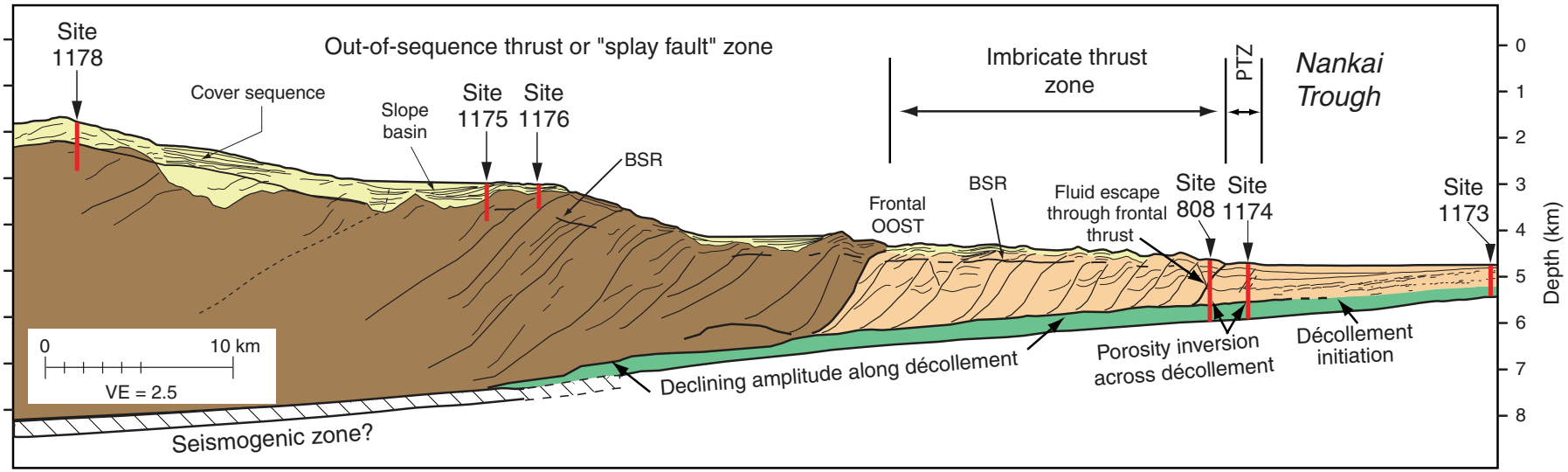

Figure F3. Lower hemisphere stereographic projection of poles to faults and fractures from resistivity-at-the-bit (RAB) imaging at Site 1173 (Shipboard Scientific Party 2001a). Offsets, where observed, were all normal.

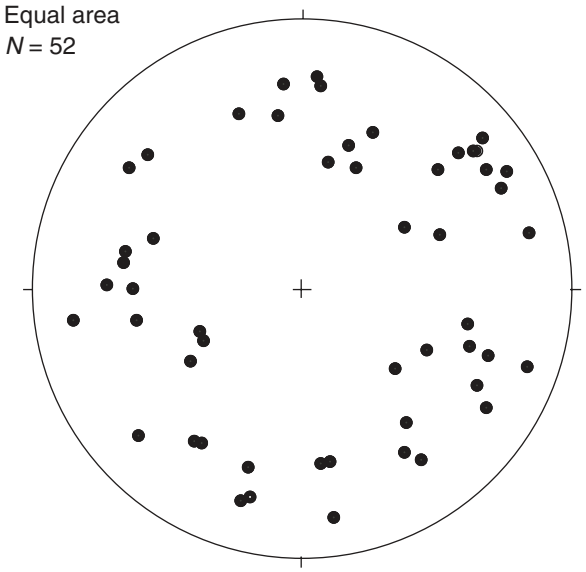

Figure F4. Two-way traveltime to subducting oceanic basement showing horst and graben structures (Heffernan et al., 2004). Colored region represents the extent of the 3-D survey. Thin red lines denote fault segments derived from a dip map on a horizon in the upper Shikoku Basin unit. All faults are normal when examined in vertical section of 3-D seismic data. Heavy red line denotes trace of the frontal thrust, with teeth on the overriding accretionary wedge. Black lines outline prominent structural trends interpreted to be relict seafloor spreading fabric. Rose diagrams of fault orientations are shown for all faults (upper right), faults overlying basement structural highs (lower right), and faults overlying basement structural lows (upper left). Faults and fractures at Site 1173 (Fig. F3, p. 18) appear more random than the segments mapped seismically, perhaps due to undersampling of the former.

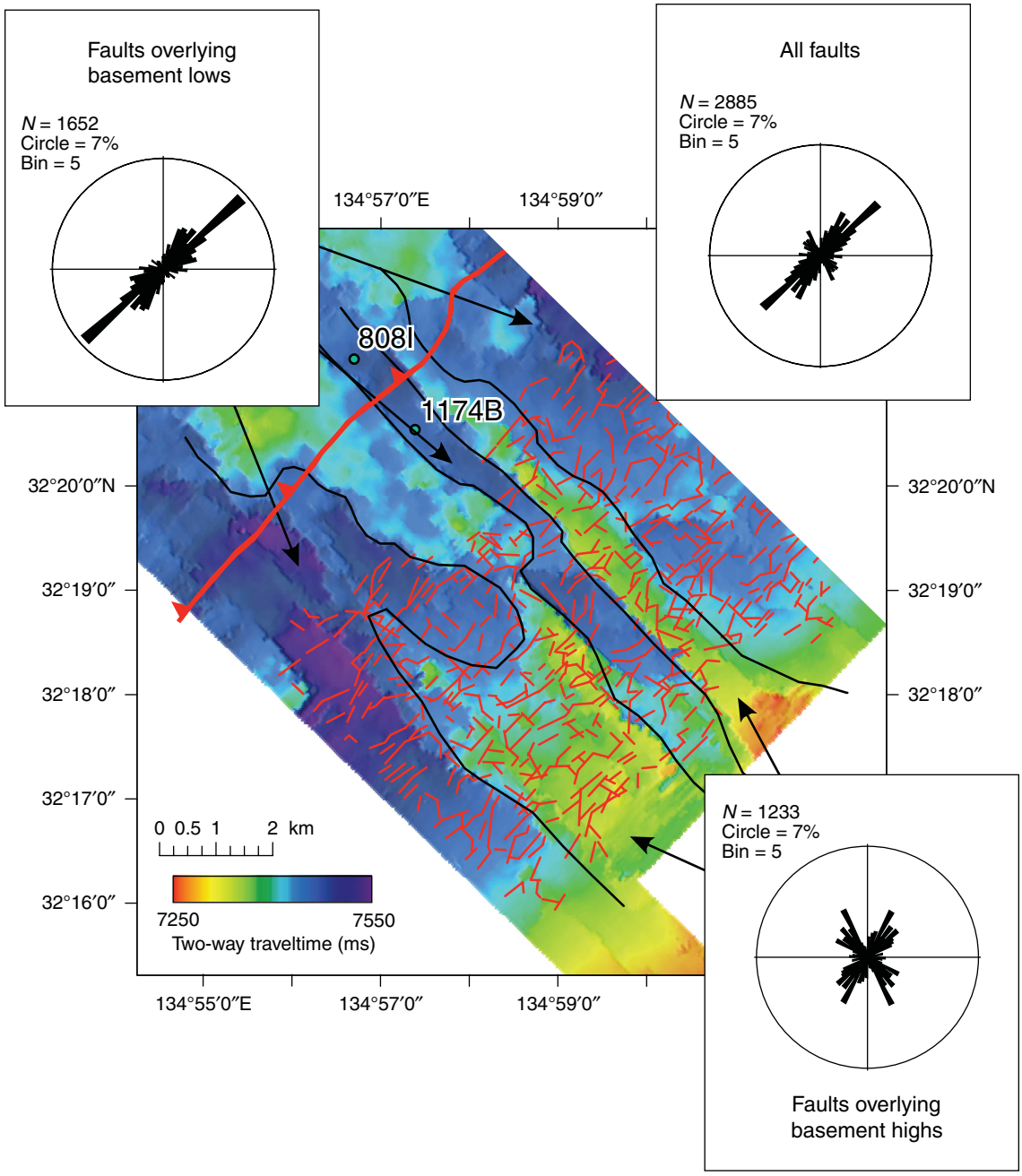

Figure F5. Seismic and interpretive sections illustrating stratigraphy and structure of the prism toe of the Muroto Transect area (after Heffernan, et al., 2004). This seismic line is through the middle of the 3-D seismic volume and is approximately along the line shown on Figure F1, p. 16. Sections are perpendicular to the trench axis and parallel to the direction of convergence. Fault 1 is the prominent protothrust. Fault 2 is the frontal thrust. Faults 3 and 4 are older in-sequence imbricate thrusts. Numerous small-offset normal faults are visible in the upper and middle part of the incoming Shikoku Basin sequence. The convergence-related "deformation front" is defined by initial thickening and deformation of the trench fill. The deformation is commonly not resolvable seismically, but indicated by thickening and uplift. The deformation front is also reflected in a change to a subtle seaward tilt of the trench floor. The décollement zone can be recognized as a bright reflector extending at least to and locally beyond the seaward limit of the deformation front. VE = vertical exaggeration.

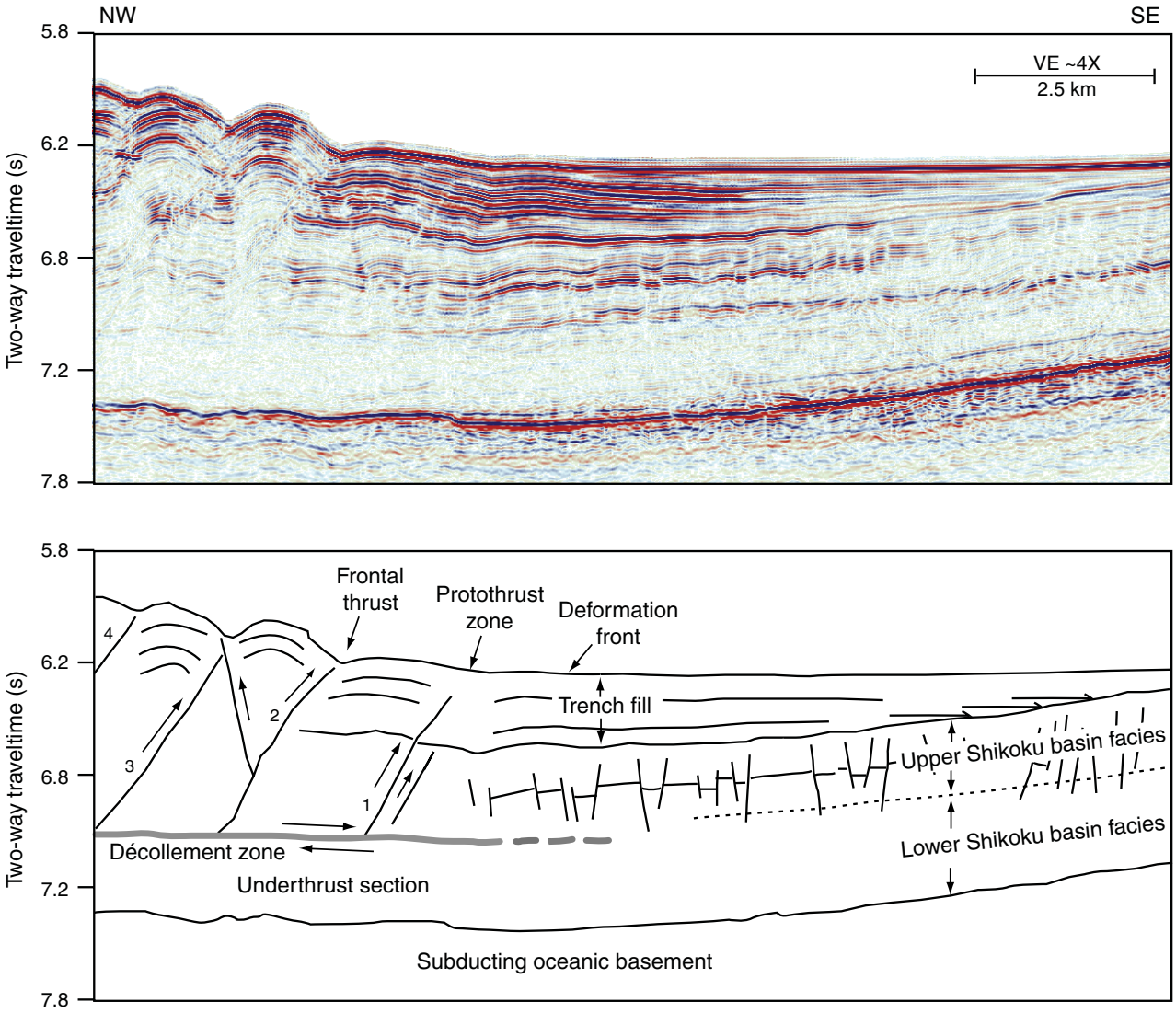

Figure F6. Static normalized resistivity-at-the-bit image within trench fill deposits above the frontal thrust in Hole 808I (from McNeill et al., 2004). Borehole breakouts are the two dark stripes of low resistivity 180° apart, representing borehole elongation in the direction northeast-southwest (σ_2). Three images represent formation resistivity (**A**) 1, (**B**) 3, (**C**) 5 in from borehole. Deformation decreases away from the borehole. The maximum principal stress (σ_1) would be oriented northwest or 90° from the orientation of the maximum breakout direction.

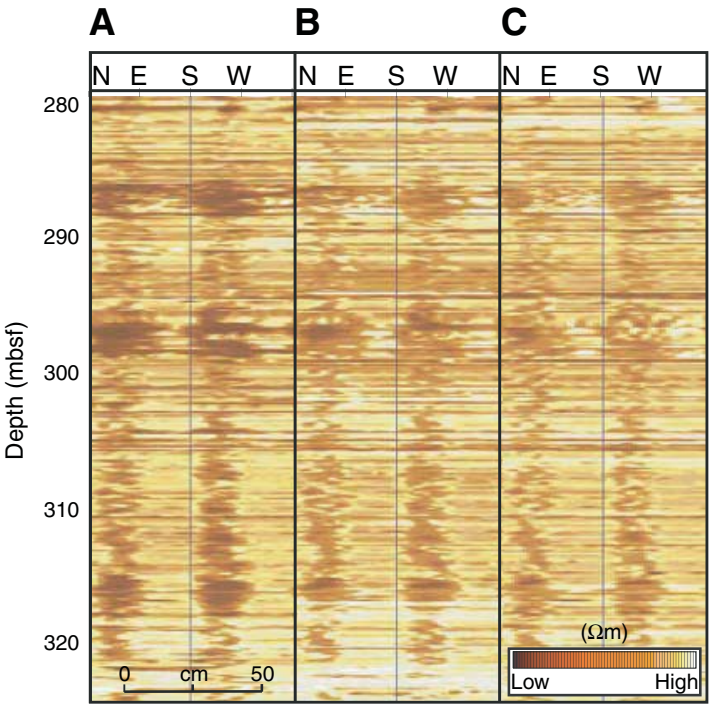

Figure F7. A schematic model of consolidation in the upper and lower Shikoku Basin facies across the trench from Sites 1173 to 1174 in the Muroto Transect (from **Bangs and Gulick,** this volume). Blue sections represent underconsolidated sediment with relatively high permeability. Dark brown represents the compacted layer that develops between the upper Shikoku Basin to lower Shikoku Basin facies boundary and the stratigraphic equivalent of the décollement zone. Arrow represents focused fluid flow. Initial trench wedge accumulation causes a compacted layer (with presumed low relative permeability) to form in the top of the lower Shikoku Basin facies as fluids are expelled and are able to move through the underconsolidated upper Shikoku Basin facies. Compaction and fluid expulsion from the upper Shikoku Basin facies midway between Site 1173 and the deformation front causes an overpressured décollement zone to develop below the compacted layer.

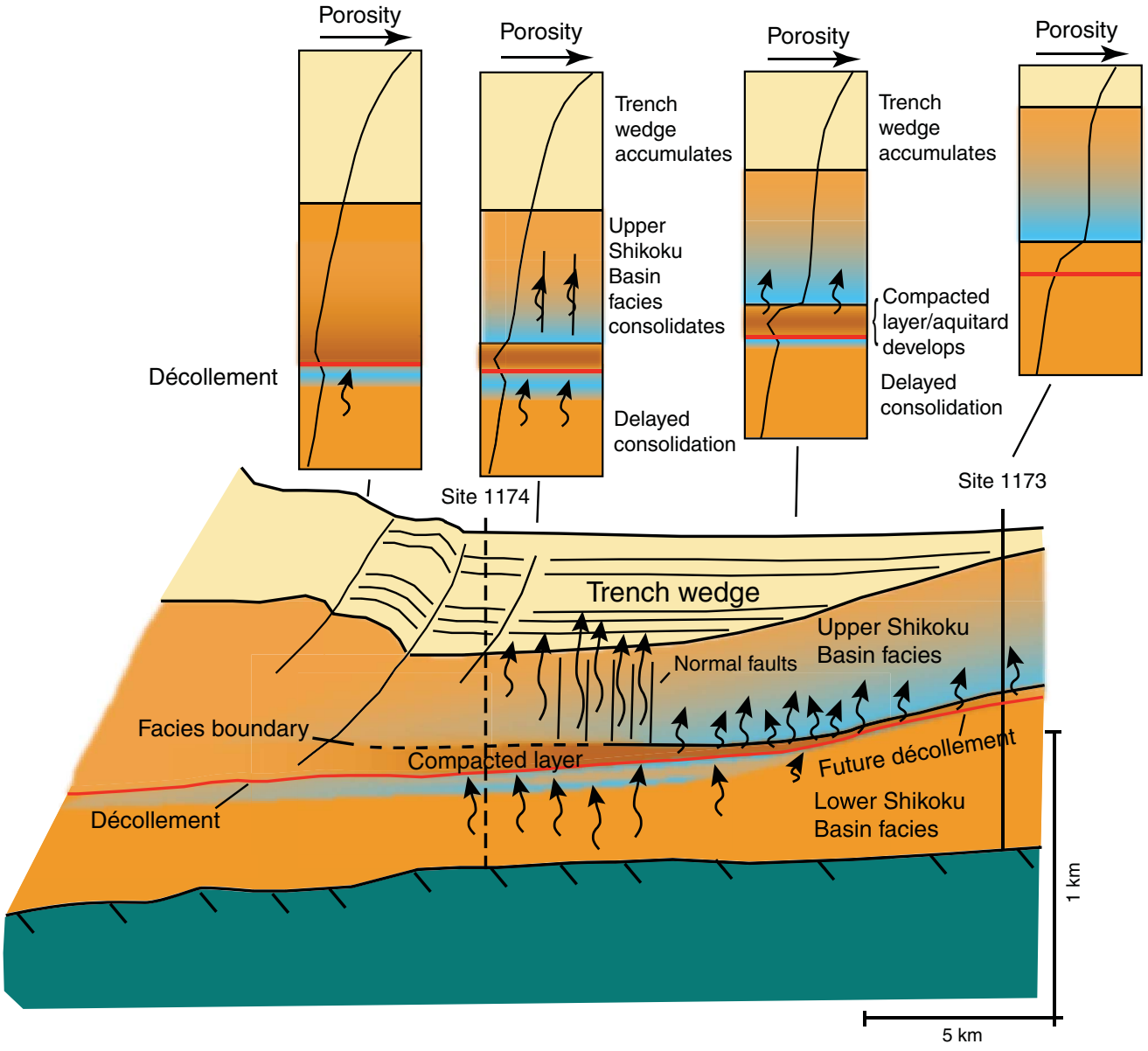

Figure F8. One-month pressure time-series (29 June to 27 July 2003) recorded by the ACORK in Hole 808I, including a major transient event. Monitoring screens are numbered from bottom to top, with the deepest screen at this site being just above the décollement (see fig. F6 of Shipboard Scientific Party, 2002a, for locations of screens). Interpretations of pressure transients, variations of seafloor loading response (dominantly tidal), and average pressures as a function of depth at Sites 808 and 1173 are under way (from Davis et al., submitted [N1]).

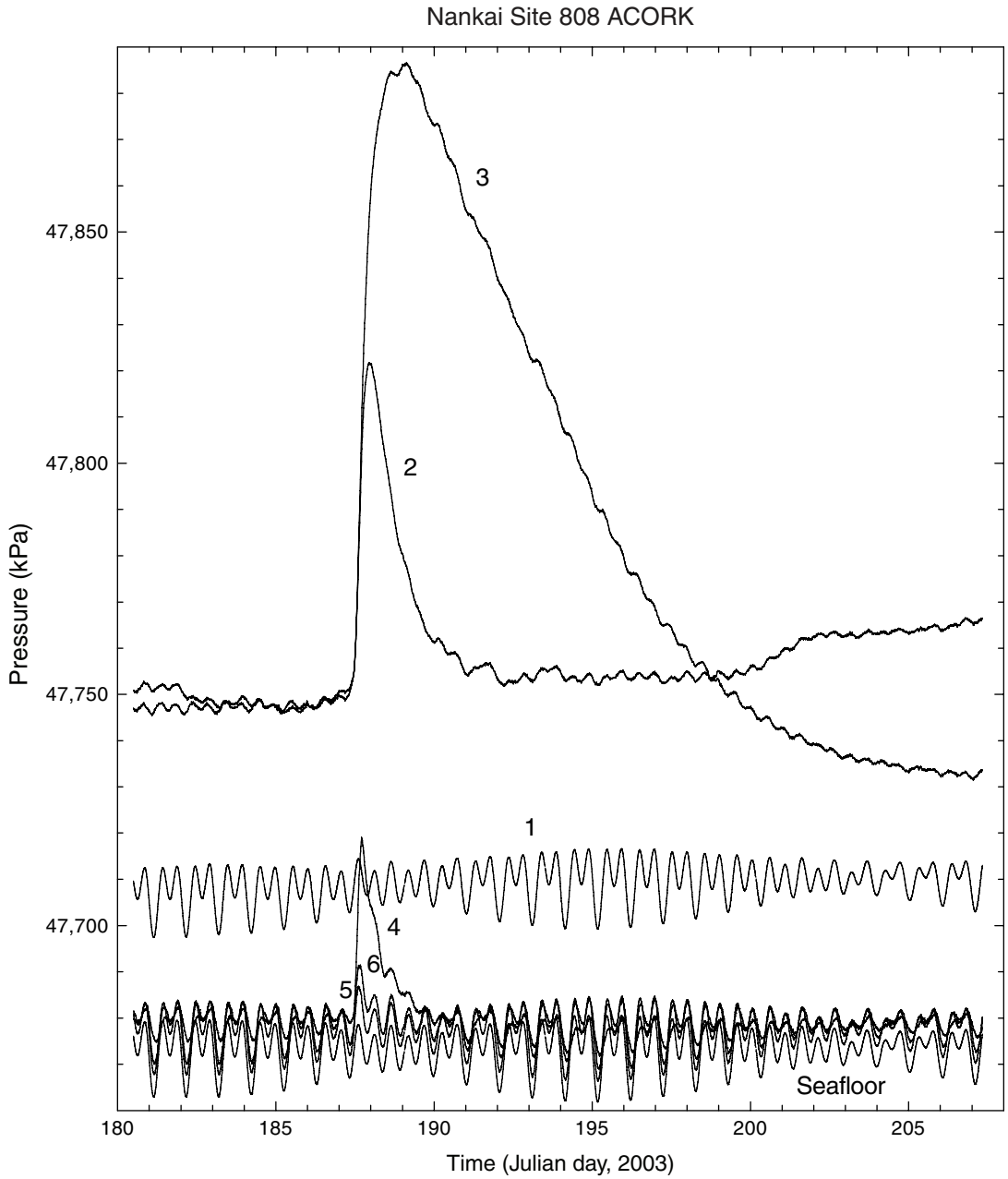

Figure F9. A series of cartoons illustrating the sedimentary and structural evolution of the central Nankai Trough of Shikoku based on DSDP/ODP Leg 87, 131, 190, and 196 data (not to scale). The subducting seamount is ~40 km in diameter at its foot and 3 km high, estimated from seismic data by Kodaira et al. (2000). The seafloor topographic highs and lows are related to the spreading fabric, transform faults, and later igneous activity associated with the final episode of Shikoku Basin spreading (north-south spreading direction) and the later near-axis Kinan Seamount igneous activity (Okino et al., 1994). The vertical height of those irregularities is ~0.5–2 km. **A.** At 7 Ma, turbidites derived from the Outer Belt of Shikoku were distributed (open arrows) into topographic lows on the Shikoku Basin floor. The topographic highs with relatively flat summits were covered by hemipelagic sediments. The subduction of the Shikoku Basin was presumed to have started at ~8 Ma, and the landward slope of the Nankai trough is mostly composed of the old accretionary prism (Shimanto Belt). **B.** At 4 Ma, accretion of the turbidites had built a substantial accretionary prism (sampled at Site 1178). The supply of the turbidites from the Outer Belt (open arrows) continued through that time as the seamount approached the trench. (Continued on next page.)

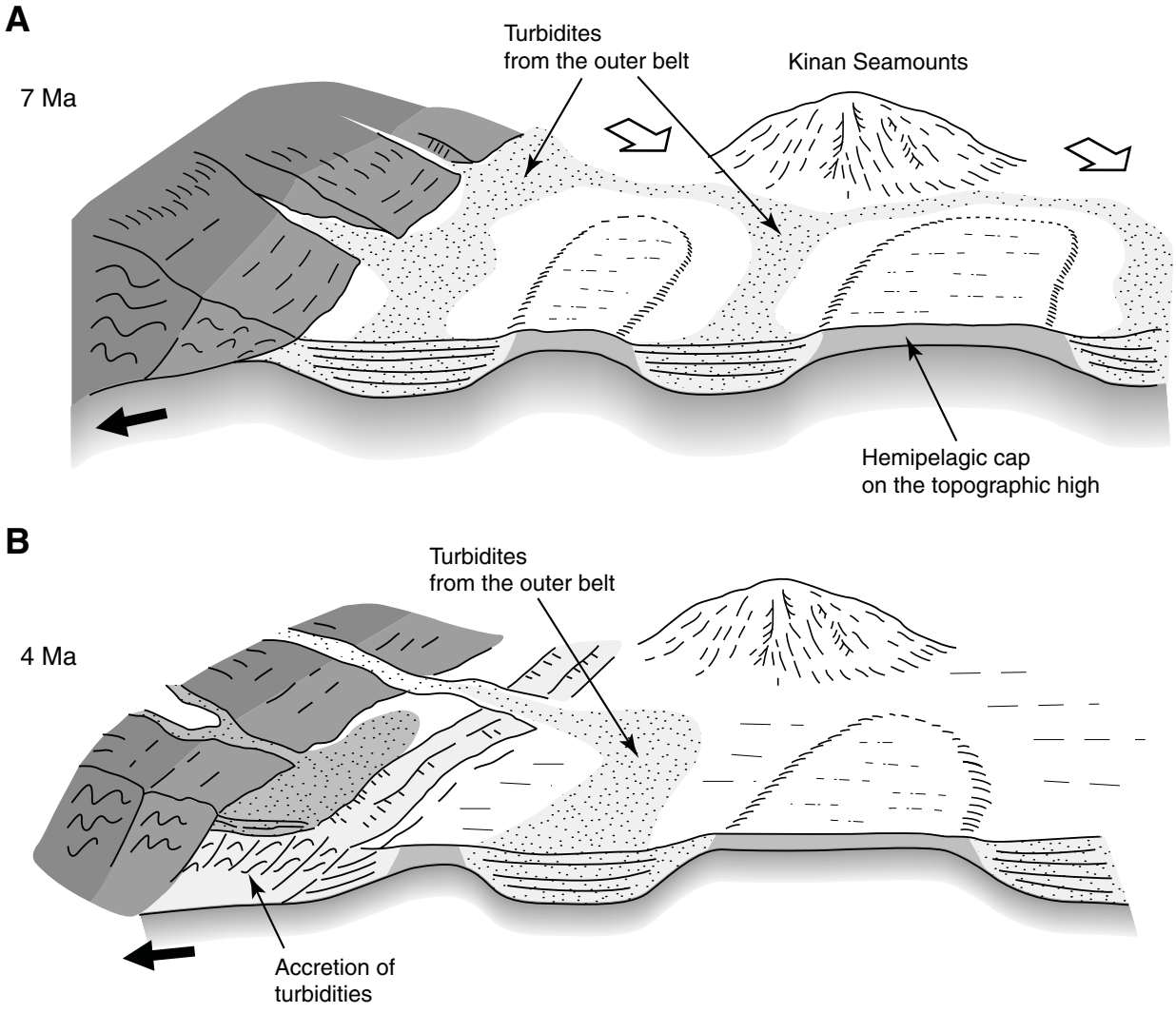

Figure F9 (continued). **C.** By 2 Ma, accretion of the turbidites from the Outer Belt was complete (sampled at Sites 1175 and 1176). The collision of the seamount had created an indentation of the accretionary prism just northeast of the Muroto Transect. A major shift of trench turbidite provenance took place at ~2 Ma and axially fed turbidites from the Izu-collision zone in the central Japan started to fill the trench axis. **D.** From 2 Ma to present, rapid accretion of axial trench turbidites dominated at Sites 808 and 1174. Subduction of the topographic high along the Muroto Transect has changed the style of deformation in the accretionary prism because it lacks a thick turbidite section, being covered instead with relatively thin hemipelagics (Sites 808, 1173, and 1174). The seamount to the north has been subducted beneath the accretionary prism, producing a large embayment. The locations of the Leg 190 and 196 drill sites are shown in their present structural setting.

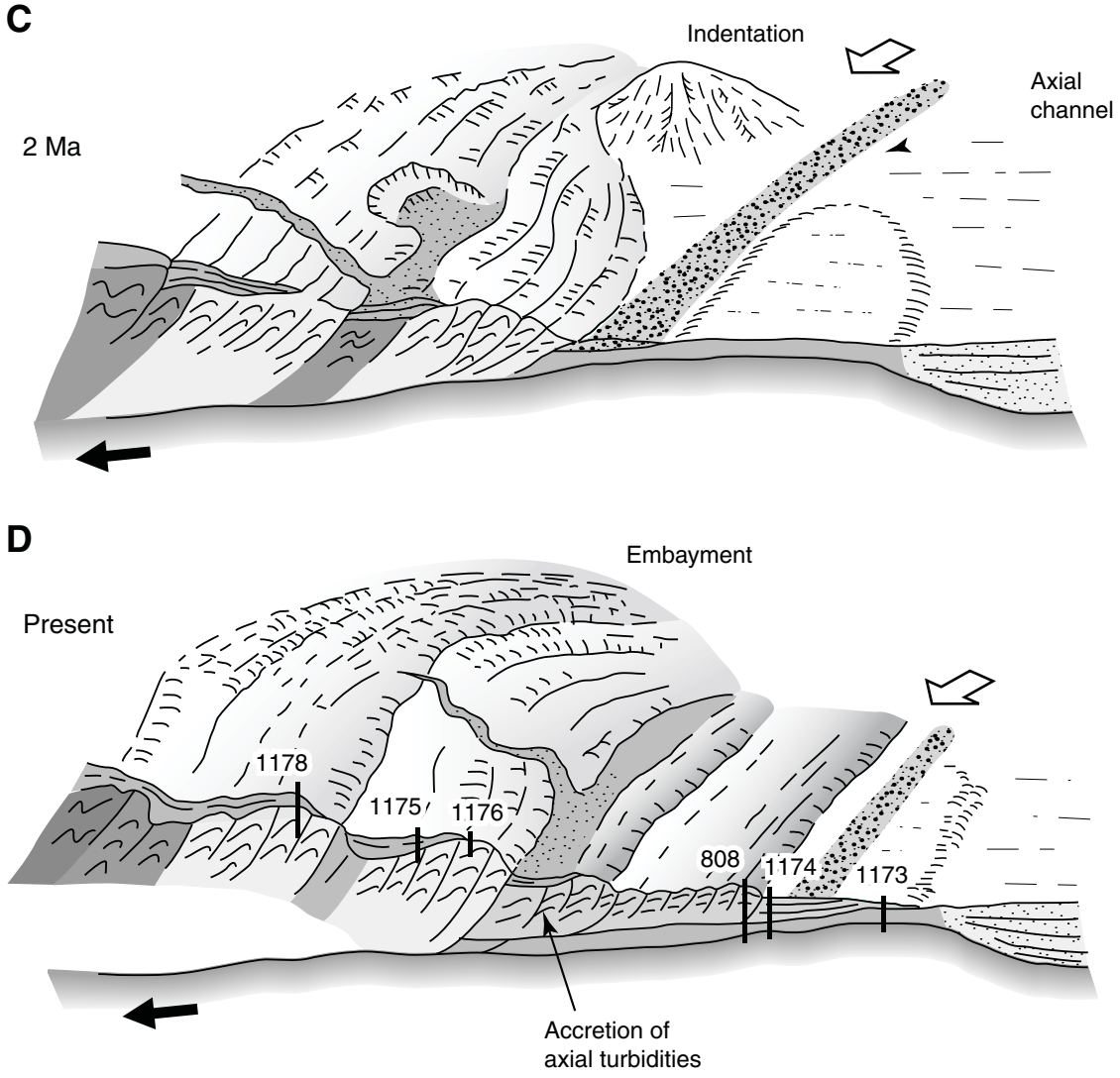

CHAPTER NOTE*

N1. Davis, E.E., Becker, K., Wang, K., Obara, K., Ito, Y., and Kinoshita, M., submitted. A discrete episode of seismic and aseismic deformation of the Nankai subduction zone accretionary prism and incoming Philippine Sea plate. *Earth Planet. Sci. Lett.*

*Dates reflect file corrections or revisions.